

Hot carriers in an intrinsic graphene

O.G. Balev

Departamento de Física, Universidade Federal do Amazonas, Manaus, 69077-000, Brazil

F.T. Vasko*

Institute of Semiconductor Physics, NAS of Ukraine, Pr. Nauki 41, Kiev, 03028, Ukraine

V. Ryzhii

*University of Aizu, Ikki-machi, Aizu-Wakamatsu 965-8580, Japan and
Japan Science and Technology Agency, CREST, Tokyo 107-0075, Japan*

(Dated: June 14, 2018)

Heating of carriers in an intrinsic graphene under dc electric field is considered taking into account the intraband energy relaxation due to acoustic phonon scattering and the interband generation-recombination transitions due to thermal radiation. The distribution of nonequilibrium carriers is obtained for the cases when the intercarrier scattering is unessential and when the carrier-carrier Coulomb scattering effectively establishes the quasiequilibrium distribution with the temperature and the density of carriers that are determined by the balance equations. Because of an interplay between weak energy relaxation and generation-recombination processes a very low threshold of nonlinear response takes place. The nonlinear current-voltage characteristics are calculated for the case of the momentum relaxation caused by the elastic scattering. Obtained current-voltage characteristics show low threshold of nonlinear behavior and appearance of the second ohmic region, for strong fields.

PACS numbers: 73.50.Fq, 81.05.Uw

I. INTRODUCTION

Active study of graphene, taking place in recent years, is stimulated both by unusual physical properties of this gapless and massless semiconductor (see discussion and references in the review [1]) and by the need to study the possibilities of applications in electronics, see discussion in [2]. For such applications study of a response of nonequilibrium carries is important and very much needed. Both experimental and theoretical studies of the nonequilibrium electron-hole pairs in graphene under interband photoexcitation have been already performed, see [3] and [4, 5] (and references therein), respectively. Experimental investigations of the carries heating in graphene by dc electric field were carried out in relation with demonstrations of graphene field-effect transistor (see [6] and references therein). Essential heating apparently had taken place in experiments on current-induced cleaning of graphene [7]. In respect to theoretical treatments of the problem, it was investigated the rate of energy relaxation of nonequilibrium carries, both analytically [8] and numerically, [9] and also it was discussed a derivation of kinetic equation for a strong field [10]. However, to the best of our knowledge, the basic problem of carries heating by dc electric field have not been considered so far and a systematic investigation of the non-linear current-voltage characteristics was not performed yet.

In this paper, we study a heating of electron-hole pairs in an intrinsic graphene under dc electric field. To describe heating it is taken into account both increase of the energy of carries in the field, \mathbf{E} , and the following relaxation processes: (1) damping of the momentum due to elastic scattering on structural disorder, that is the most fast process ensuring weak anisotropy of the distribution function [11], (2) intraband quasi-elastic energy relaxation on acoustic phonons, (3) generation-recombination processes due to interband transitions induced by thermal radiation, and (4) intercarrier scattering due to Coulomb interaction. In present study we consider the heating within two limiting regimes: (*I*) if the Coulomb scattering is unessential, when it is possible to neglect by the intercarrier scattering, and (*II*) the Coulomb-controlled case. In the latter case the Coulomb scattering imposes the quasiequilibrium distribution on carries, with characteristics defined by balance equations for the density and the energy. In present study we find the distribution function of carries for these regimes and investigate it dependence on applied field and the temperature of thermostat formed by phonons and thermal radiation. In addition, we analyze current-voltage characteristics and the density of nonequilibrium carriers.

The character of obtained nonlinear response is determined by a few peculiarities of the considered model. First, the velocity of carries does not increase with the energy as it is equal $v_W \mathbf{p}/p$, where $v_W = 10^8$ cm/s is the characteristic velocity of charged neutrino-like particles, \mathbf{p} is the 2D momentum. Second, the interband transitions are effectively excited by thermal radiation (the matrix element of transition is $\propto v_W$) they not only

*Electronic address: ftvasko@yahoo.com

change a carrier concentration but also participate in the energy relaxation. As a result, the nonequilibrium distribution is formed due to interplay between weak energy relaxation and generation-recombination processes (i.e., between interactions with phonon and photon thermostats). Third, the rate of energy relaxation sharply increases as p grows, where weak electron-phonon interaction takes place for slow carriers. Therefore for scattering on short-range defects, when the relaxation of momentum also grows with the energy, it is realized a sub-linear current-voltage characteristic with essential nonlinearity for weak fields while as field grows nonlinearity becomes weak. If the momentum relaxation becomes ineffective for high energy carriers (because of a finite-range disorder) a super-linear increase of current takes place. In the region of strong fields a linear dependence of current from the field is realized (the second ohmic region of current-voltage characteristic) where the effective conductivity is smaller than the conductivity of equilibrium carriers for low temperatures, T , and the former becomes larger than the latter as T grows. Because the intrinsic graphene has maximum resistance (with respect to gate voltage), here the Joule heating is least effective so maximal electric field can be applied.

The paper is organized in the following way. The basic equations describing the heating of carriers in an intrinsic graphene under dc electric field are presented in Sec. II. In Sec. III we examine the symmetric distribution function of nonequilibrium electron-hole pairs for the cases I and (II) , see above. The current-voltage characteristics are analyzed in Sec. IV. The concluding remarks and discussion of the assumptions used are given in the last section. Appendix contains the evaluation of the quasi-classical kinetic equation for electron-hole pairs under a strong dc electric field.

II. BASIC EQUATIONS

Nonequilibrium electron-hole pairs in the intrinsic graphene are described by coinciding distribution functions $f_{e,h\mathbf{p}} \equiv f_{\mathbf{p}}$ as their energy spectra are symmetric and processes of scattering there are identical (see Appendix). Therefore instead of system of kinetic equations for $f_{e\mathbf{p}}$ and $f_{h\mathbf{p}}$ it is possible to consider the single kinetic equation as

$$e\mathbf{E} \cdot \frac{\partial f_{\mathbf{p}}}{\partial \mathbf{p}} = \sum_j J_j \{f|\mathbf{p}\}, \quad (1)$$

where \mathbf{E} is a strong electric field and the classical form of the field term is substantiated in Appendix. Here \mathbf{p} is the 2D momentum and $J_j \{f|\mathbf{p}\}$ is the collision integral for the j th scattering mechanism, with index $j = D, LA, R,$ and C correspond to the static disorder (D), the acoustic phonon scattering (LA), the radiative-induced interband transitions (R), and the carrier-carrier scattering (C), respectively. Integrals of elastic scatter-

ing there were considered earlier, see [11, 12] and references therein, $J_{LA} \{f|\mathbf{p}\}$ and $J_R \{f|\mathbf{p}\}$ were evaluated in [5], and Coulomb scattering was considered in [13]. For the distribution function defined by Eq. (1), the concentration balance equation is given as

$$\frac{4}{L^2} \sum_{\mathbf{p}} J_R \{f|\mathbf{p}\} = 0, \quad (2)$$

because interband transitions are forbidden not only for elastic scattering but also for Coulomb scattering, due to symmetry of the energy spectrum [14], and for phonon scattering, due to $s \ll v_W$; here s is the velocity of sound. In Eq. (2) the factor 4 takes into account spin and valley degeneracies, L^2 is the normalization area.

Taking into account that electrons and holes equally contribute to the current density, \mathbf{I} , one obtains

$$\mathbf{I} = \frac{8ev_{BW}}{L^2} \sum_{\mathbf{p}} \frac{\mathbf{p}}{p} \Delta f_{\mathbf{p}}, \quad (3)$$

where the asymmetric part of distribution function, $\Delta f_{\mathbf{p}}$, is separated from the symmetric one, f_p , by using the relation $f_{\mathbf{p}} = f_p + \Delta f_{\mathbf{p}}$. Last contribution is small if usual condition $|e\mathbf{E}|\tau_p^{B(m)} \ll p$ is satisfied. [15] Here $\tau_p^{B(m)}$ is the momentum relaxation time and $\Delta f_{\mathbf{p}}$ is given as

$$\Delta f_{\mathbf{p}} = \frac{(e\mathbf{E} \cdot \mathbf{p})}{p} \tau_p^{B(m)} \left(-\frac{df_p}{dp} \right). \quad (4)$$

For the case of a random potential $U_{\mathbf{x}}$ characterized by the correlation function $\langle U_{\mathbf{x}} U_{\mathbf{x}'} \rangle \equiv \overline{U_d^2} \exp\{-[(\mathbf{x} - \mathbf{x}')/l_c]^2\}$ with the averaged energy $\overline{U_d}$ and the correlation length l_c , one obtains [11]

$$\frac{1}{\tau_p^{B(m)}} = \frac{v_d p}{\hbar} \Psi \left(\frac{pl_c}{\hbar} \right), \quad \Psi(z) = \frac{e^{-z^2}}{z^2} I_1(z^2), \quad (5)$$

where the decreasing with pl_c/\hbar form-factor $\Psi(z)$ is written through the modified Bessel function $I_1(x)$ and the characteristic velocity v_d is introduced as $v_d = \pi \overline{U_d^2} l_c^2 / 4\hbar^2 v_W$. The conductivity, σ is determined according to the standard formula $\mathbf{I} = \sigma \mathbf{E}$. Using the above-introduced relaxation time (5) and Eqs. (3, 4), one transforms the conductivity as follows

$$\sigma = \frac{e^2}{\pi \hbar} \frac{2v_W}{v_d} \int_0^\infty \frac{dp}{\Psi(pl_c/\hbar)} \left(-\frac{df_p}{dp} \right), \quad (6)$$

where the averaging over angle is performed.

Further, we turn to the averaging over angle (below we symbolize such averaging as a line over expression) of Eq. (1). Neglecting the weak contribution of $\Delta f_{\mathbf{p}}$ in the right-hand side of (1), one obtains the kinetic equation for symmetric distribution f_p in the following form

$$\overline{e\mathbf{E} \cdot \frac{\partial \Delta f_{\mathbf{p}}}{\partial \mathbf{p}}} = \sum_j \overline{J_j \{f|p\}}. \quad (7)$$

Here $J_j\{f|p\} = \overline{J_j\{t|\mathbf{p}\}}$ and summation is performed over $j = LA, R, C$ because the elastic scattering does not affect the symmetric distribution due to the energy conservation. Performing the averaging over the angle, we transform the field contribution of Eq. (7) as follows [16]

$$e\mathbf{E} \cdot \frac{\partial \Delta f_{\mathbf{p}}}{\partial \mathbf{p}} = \frac{(eE)^2}{2p} \frac{d}{dp} p_T^{\beta(m)} \left(-\frac{df_p}{dp} \right). \quad (8)$$

As a result, using the Fokker-Planck form of $J_{LA}\{f|p\}$ and $J_{BR}\{f|p\}$ obtained in [5], we arrive to kinetic equation

$$\frac{\nu_p^{\beta(qe)}}{p^2} \frac{d}{dp} \left\{ \left[p^4 + \frac{p_E^4}{2\Psi(pl_c/\hbar)} \right] \frac{df_p}{dp} + \frac{p^4}{p_T} f_p(1-f_p) \right\} + \nu_p^{\beta(R)} [N_{2p/p_{BT}}(1-2f_p) - f_p^2] + J_{BC}\{f|p\} = 0, \quad (9)$$

where $N_x = (e^x - 1)^{-1}$ is the Planck distribution and $p_T = T/v_W$. The rates of quasi-elastic energy relaxation, $\nu_p^{\beta(qe)}$, and of radiative transitions, $\nu_p^{\beta(R)}$, can be presented in the form [5]

$$\nu_p^{\beta(qe)} = \left(\frac{s}{v_W} \right)^2 \frac{v_{ac} p}{\hbar}, \quad v_{ac} = \frac{D^2 T}{4\hbar^2 \rho_s v_W s^2},$$

$$\nu_p^{\beta(R)} = \frac{v_r p}{\hbar}, \quad v_r = \frac{e^2 \sqrt{\epsilon}}{\hbar c} \left(\frac{v_w}{c} \right)^2 \frac{8v_W}{3}. \quad (10)$$

The characteristic velocities v_{ac} and v_r are introduced here in order to separate the linear momentum dependence and expressed through the deformation potential and the sheet density of graphene, D and ρ_s , as well as the dielectric permittivity, ϵ . Characteristic momentum, p_E , is defined in Eq. (9) by relation

$$p_E^4 = \left(\frac{v_W}{s} \right)^2 \frac{(eE\hbar)^2}{v_{ac} v_d}, \quad (11)$$

so that $p_E \propto \sqrt{E}$. The Coulomb scattering integral $J_C\{f|p\}$ can be neglected in Eq. (9) for the case *I* therefore here nonequilibrium distribution f_p is defined by nonlinear differential equation of the second order.

For other approach, in the case *II*, the Coulomb scattering term in Eq. (9) is dominant and it imposes quasiequilibrium distribution

$$\tilde{f}_p = \{ \exp[(v_W p - \mu)/T_c] + 1 \}^{-1}, \quad (12)$$

with effective temperature of carriers T_c and quasichemical potential μ . To determine T_c and μ we will use the concentration balance equation (2) and the energy balance equation. The latter we obtain by summing of Eq. (7) over \mathbf{p} with the energy weight $v_W p$ as follows

$$\frac{1}{2} \sigma E^2 + \frac{4v_W}{L^2} \sum_{\mathbf{p}} p [J_{LA}(f|p) + J_R(f|p)] = 0, \quad (13)$$

where the field term is expressed through the conductivity (6) using the integration by parts (the factor 1/2 is

quite understood as the total Joule heat σE^2 must to be divided equally between electrons and holes). Therefore, the two parameters of \tilde{f}_p are determined by two transcendent equations (2) and (13). Now, the nonlinear conductivity should be calculated under substitution \tilde{f}_p into Eq. (6).

III. NONEQUILIBRIUM DISTRIBUTION

Below we consider the nonequilibrium distribution obtained from Eq. (9) with the Coulomb contribution omitted (case *I*) or from the balance equations (2) and (13) (case *II*). Also we present the field and temperature dependencies of the nonequilibrium sheet concentration.

A. Weak intercarrier scattering

We start with consideration of the case *I*, when the carrier-carrier scattering is ineffective. Omitting J_C in Eq. (9) and introducing the dimensionless momentum $x = p/p_T$ and the parameter $\eta = p_T l_c / \hbar$, we obtain the nonlinear differential equation

$$\frac{d}{dx} \left\{ \left[x^4 + \frac{(p_E/p_T)^4}{2\Psi(x\eta)} \right] \frac{df_x}{dx} + x^4 f_x(1-f_x) \right\} + \Gamma x^2 \left(\frac{1-2f_x}{e^{2x}-1} - f_x^2 \right) = 0. \quad (14)$$

Here the dimensionless parameter $\Gamma = (v_W/s)^2 v_r / v_{ac}$ determines the ratio of contributions from the thermal radiation and acoustic phonons, to the energy relaxation. As the boundary conditions for Eq. (14) we use that $x^4(df_x/dx + f_x)_{x \rightarrow \infty} = 0$, so that f_x must decrease for $x \rightarrow \infty$ sufficiently fast, and also the density balance equation (2). [15] If to integrate Eq. (14) over x from 0 to ∞ , then for finite electric field besides Eq. (2) we obtain additional, proportional to $(p_E/p_T)^4 (df_x/dx)_{x=0}$, term that, certainly, must be equal to zero. Thus, instead of Eq. (2), the second boundary condition can be used in the following form $(df_x/dx)_{x \rightarrow 0} = 0$.

The numerical solution of Eq. (14) is performed below with the use of the finite difference method and the iterations over non-linear contributions, see [17]. Distribution functions obtained are presented in Figs. 1 and 2 as functions of the energy for different temperatures, electric fields, and l_c . For low temperature region, two regimes of the modification of a distribution emerge with the increase of field: weak electric fields, $(p_E/p_T)^4 / (4\Gamma) \ll 1$, and strong electric fields, $(p_E/p_T)^4 / (4\Gamma) \gg 1$.

As it is seen from Figs. 1a and 2 in weak fields there is essential suppression of the distribution in the region of small $p < p_T$ (as slow carriers are heated very effectively) and for large $p > p_T$ distribution remains almost equilibrium one. Further, as the field becomes strong, Figs. 1 and 2 show that the carriers are spread over a wide region of energies such that, e.g., at $T=4.2$ K for $E > 5$ V/cm the

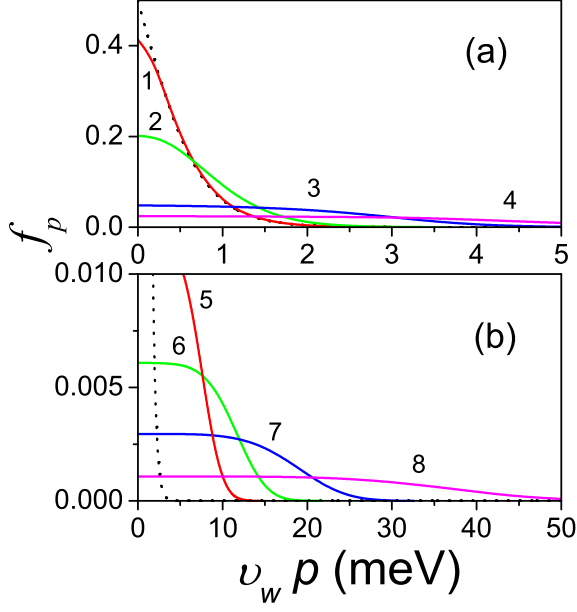


FIG. 1: (Color online) Determined from Eq. (14) distribution functions, at $T=4.2$ K and $l_c=10$ nm: (a) for weak electric fields $E=0.1$ mV/cm (1), 1 mV/cm (2), 10 mV/cm (3), and 30 mV/cm (4); (b) for strong electric fields $E=0.1$ V/cm (5), 0.3 V/cm (6), 1 V/cm (7), and 5 V/cm (8). Dotted curves correspond to the equilibrium distribution.

tail of the distribution will reach the energies for which the spontaneous emission of the optical phonons begins (~ 90 meV). It is seen, as well in agreement with Figs. 1 and 2, that with the increase of T the transition between the weak field and the strong field regimes occurs at a higher $E \propto T^2$. In Figs. 2a - 2c we plot the distribution functions for $l_c=10$ nm and 20 nm for different E and T . It is seen that with the increase of E the influence of a finite l_c grows, by making the effect of electric field on the distribution function more pronounced for higher l_c . However, for weak E the difference between the solid curve and its dashed counterpart is practically invisible. Notice, from the solid and, especially, the dashed curves 4 in Fig. 2c it follows that here interaction with optical phonons can be important.

B. Coulomb controlled distribution

Further, we examine the case *II*, when quasiequilibrium distribution Eq. (12) is determined from the balance equations, (2) and (13). Introducing dimensionless momentum, $y = v_W p / T_c$, such that $\tilde{f}_y = [\exp(y - \mu/T_c) + 1]^{-1}$, we rewrite the concentration balance equation (2) in the form

$$\int_0^\infty dy y^2 \left(\frac{1 - 2\tilde{f}_y}{e^{2yT_c/T} - 1} - \tilde{f}_y^2 \right) = 0, \quad (15)$$

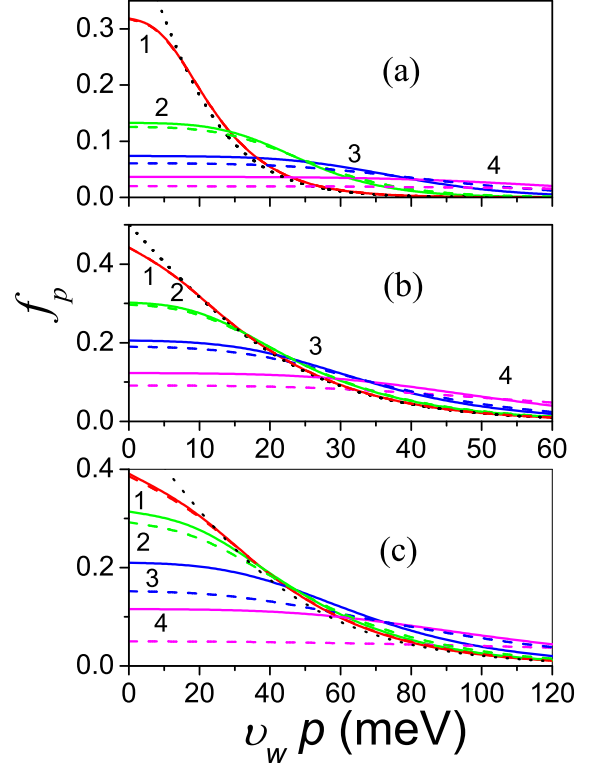


FIG. 2: (Color online) The same as in Fig. 1 calculated: (a) for $T=77$ K and $E=0.14$ V/cm (1), 1.4 V/cm (2), 4.4 V/cm (3), and 14 V/cm (4); (b) for $T=150$ K and $E=74$ mV/cm (1), 0.74 V/cm (2), 2.35 V/cm (3), and 7.4 V/cm (4); (c) for $T=300$ K and $E=1$ V/cm (1), 3 V/cm (2), 10 V/cm (3), and 30 V/cm (4). The solid and the dashed curves correspond to $l_c=10$ nm and 20 nm, respectively. Dotted curves correspond to equilibrium distributions.

which gives the relation between μ/T and dimensionless temperature T_c/T (this relation is not dependent explicitly on the field). Now the energy balance equation (13) is given as

$$Q_E - \frac{T_c - T}{T} \int_0^\infty dy y^4 e^{y - \mu/T_c} \tilde{f}_y^2 + \Gamma \int_0^\infty dy y^3 \left(\frac{1 - 2\tilde{f}_y}{e^{2yT_c/T} - 1} - \tilde{f}_y^2 \right) = 0, \quad (16)$$

where field contribution Q_E is transformed using Eq. (6)

$$Q_E = \left(\frac{pE}{T_c/v_W} \right)^4 \left[\tilde{f}_{y=0} + \frac{\eta_c}{2} \int_0^\infty dy \tilde{f}_y \Phi(\eta_c y) \right]. \quad (17)$$

Here $\eta_c = T_c l_c / \hbar v_W$ and it is introduced the function $\Phi(z) = -\Psi'(z)/\Psi(z)^2$ and taken into account that $\Psi(0) = 1/2$.

In Figs. 3a and 3b calculated from Eqs. (15), (16) dimensionless effective temperature T_c/T and maximal

value of the distribution function $\tilde{f}_{p=0} = [\exp(-\mu/T_c) + 1]^{-1}$, that determines quasichemical potential, are shown as function of E for different T . From Fig. 3a it is seen that T_c/T grows faster with the increase of E for larger l_c ; in addition, the grows of dimensionless effective temperature becomes faster for smaller T . Figure 3b shows that the characteristic value of distribution, $f_{p=0}$, decreases faster with E at smaller T .

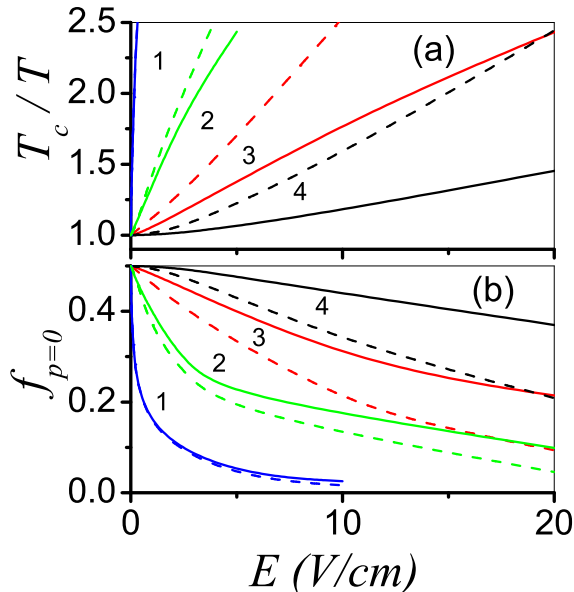


FIG. 3: (Color online) Determined from the balance Eqs. (15), (16) dimensionless effective temperature T_c/T (a) and maximal distribution $\tilde{f}_{p=0}$ (b) versus electric field for $T = 20$ K (1), 77 K (2), 150 K (3), and 300 K (4). Solid and dashed curves are correspondent to $l_c = 10$ nm and 20 nm, respectively.

C. Hot carrier concentration

Using the solutions of Eq. (14) or of the balance Eqs. (15)-(17), we calculate below the sheet concentration which is determined as follows

$$n = \frac{2}{\pi\hbar^2} \int_0^\infty dp p f_p. \quad (18)$$

Here in the right hand side f_p is replaced by \tilde{f}_p for the case II. As a result, the field dependence of n is determined by a competition of the effective temperature T_c grows and the maximal distribution $\tilde{f}_{p=0}$ decrease, see Figs. 3a and 3b: so that the concentration will grow slowly with the field.

In Fig. 4 we plot the dimensionless carrier concentrations n/n_T as function of E . Here the equilibrium concentration readily follows from Eq. (18) as $n_T = \pi(T/\hbar v_W)^2/6$ [notice, at $T = 4.2$ K, 20 K, 77

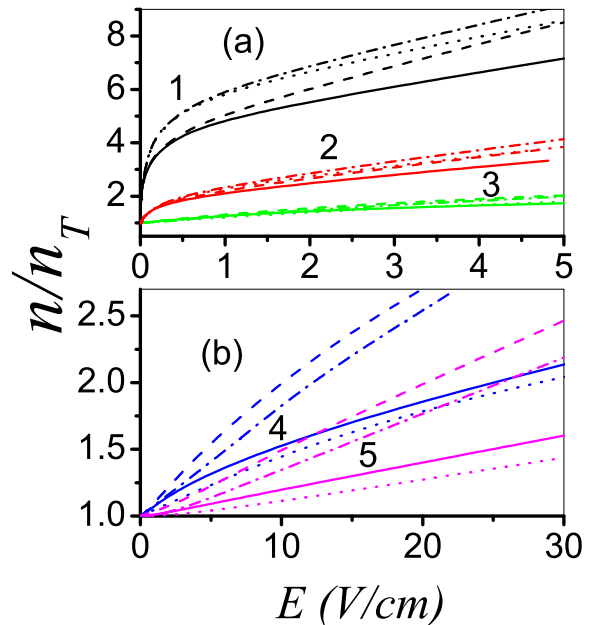


FIG. 4: (Color online) Normalized carrier concentration, n/n_T , versus electric field: (a) at $T = 4.2$ K (1), 20 K (2), 77 K (3) and (b) at $T = 150$ K (4), 300 K (5). The solid and the dashed curves are calculated from Eq. (14) for $l_c = 10$ nm and 20 nm, respectively. The dotted and the dot-dashed curves are calculated from Eqs. (15)-(17) for $l_c = 10$ nm and 20 nm, respectively.

K, 150 K, and 300 K one obtains $n_T = 1.6 \times 10^7 \text{cm}^{-2}$, $3.6 \times 10^8 \text{cm}^{-2}$, $5.4 \times 10^9 \text{cm}^{-2}$, $2.0 \times 10^{10} \text{cm}^{-2}$, and $8.1 \times 10^{10} \text{cm}^{-2}$, respectively]. From Fig. 4 it is seen that: i) at low temperatures (and not too large E) the relative increase of the density $(n - n_T)/n_T$ is approximately $\propto E^{1/2}$ as due to small characteristic momentum, \bar{p} , effect of a finite l_c is negligible; ii) at higher temperatures (or very large E) $(n - n_T)/n_T \approx A + BE$, i.e., it is linear as due to large \bar{p} effect of a finite l_c becomes essential. Notice, that the density grows becomes faster for larger l_c .

IV. CURRENT-VOLTAGE CHARACTERISTICS

Using obtained in Secs. IIIA and IIIB nonequilibrium distribution functions we calculate here nonlinear conductivity introduced by Eq. (6) and analyze modifications of the current voltage characteristics due to temperature and l_c variations. Performing the integration in Eq. (6) by parts one arrives to

$$\sigma = \sigma_0 \left[2f_{p=0} + \frac{l_c}{\hbar} \int_0^\infty dp f_p \Phi(pl_c/\hbar) \right], \quad (19)$$

where $\sigma_0 = (2v_W/v_d)e^2/\pi\hbar$ is the characteristic conductivity. For the case of short-range scattering, $\bar{p}l_c/\hbar \ll 1$

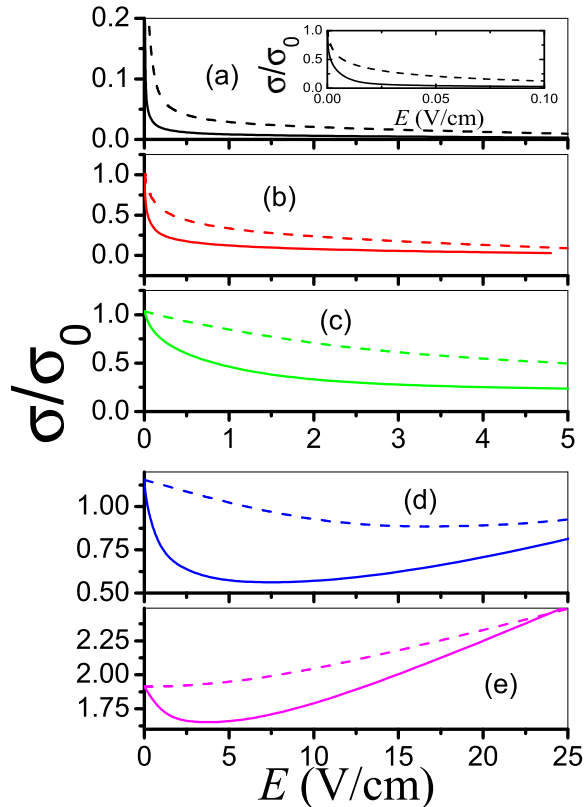


FIG. 5: Dimensionless conductivity, σ/σ_0 , versus field E for $l_c = 10$ nm at different temperatures: $T = 4.2$ K (a), 20 K (b), 77 K (c), 150 K (d), and 300 K (e). The solid and the dashed curves are calculated from Eqs. (14), (19) and Eqs. (15)-(17), (19), respectively. Inset in panel (a) shows low-field dependencies.

(\bar{p} is the characteristic momentum of hot carriers) conductivity can be expressed through the distribution function of low energy carriers as: $\sigma \simeq 2\sigma_0 f_{p=0}$. As $f_{p=0} = 1/2$ for $E \rightarrow 0$, it follows that σ_0 is the linear (in the absence of heating) conductivity in short-range scattering limit. In Fig. 5 we plot σ/σ_0 versus field E for $l_c = 10$ nm. Notice, in Figs. 5a-5c, except the inset of Fig. 5a, the same field region is used; it is different from the one used in Figs. 5d-5e. It is seen that both approaches give similar dependences even for very strong field, for given T and l_c . The dependencies σ/σ_0 vs E for $l_c = 20$ nm are plotted in Fig. 6, where conductivity grows faster for higher temperatures.

Next, we turn to consideration of the current-voltage characteristics (i.e., the current density $I = \sigma E$ versus field E). In Fig. 7 we plot the current density, $I = \sigma E$, versus field E for $l_c = 10$ nm at different temperatures. Similar dependencies for $l_c = 20$ nm are shown in Fig. 8. It is seen that current-voltage characteristics can be essentially nonlinear already for relatively small E and I starting from 10^{-5} A/cm in the low-temperature region. Point out that for larger E and I (if $E \geq 1$ V/cm at

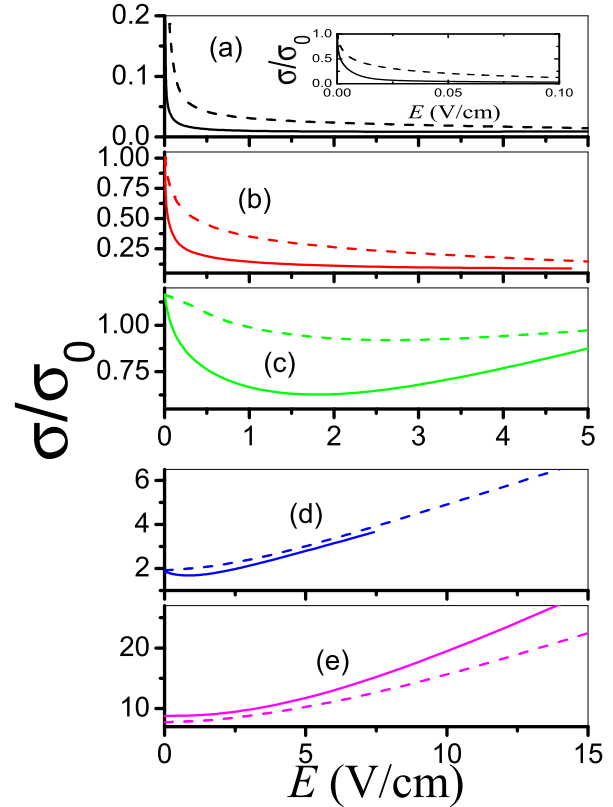


FIG. 6: The same as in Fig. 5 for $l_c = 20$ nm.

low temperatures and $E \geq 10$ V/cm at room temperature) Figs. 7 and 8 will present dependences that are close to linear ones, $A + BE$. In addition, Figs. 7 and 8 show that from both approaches (cases I and II) similar current-voltage characteristics are obtained, for given T and l_c . It is also seen that current-voltage characteristics can manifest as sublinear so superlinear form in wide E regions depending on value of T , l_c ; these modifications of the form are essentially related with the effects due to finite l_c .

V. CONCLUSIONS

To summarize, we developed the theory of the carries heating in intrinsic graphene under strong dc electric field for the cases when intercarrier scattering is negligible or dominant. It is found that the deviation from the equilibrium distribution starts from very low electric fields (from 0.3 V/cm for the room temperature and from 10 μ V/cm for the liquid helium temperature; in particular, for a finite fields df_p/dp tends to zero for $p \ll p_E \lesssim p_T$, (while for equilibrium distribution $df_p^{eq}/dp \approx -1/4pT$ has the finite constant value) due to ineffective energy relaxation of slow carriers. Since with the increase of heating this relaxation sharply grows and the recombination of carriers is dominant over the thermogeneration within the

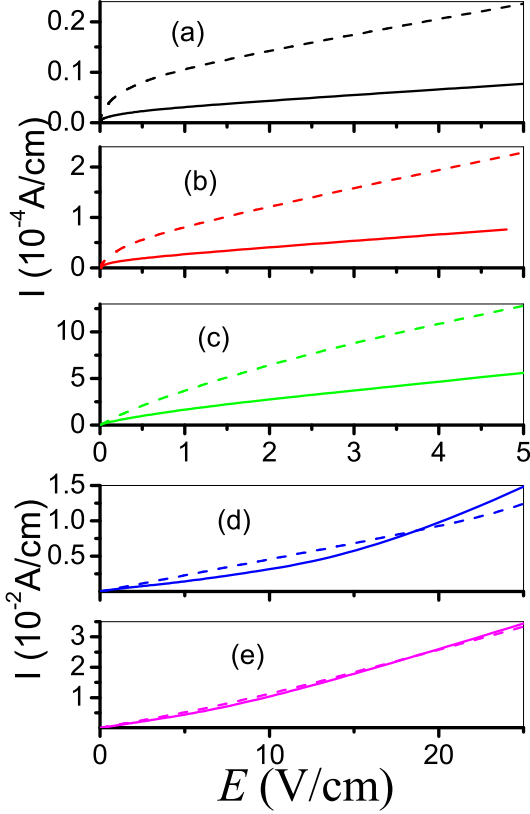


FIG. 7: Current-voltage characteristics for $l_c = 10$ nm at different temperatures: $T = 4.2$ K (a), 20 K (b), 77 K (c), 150 K (d), and 300 K (e). The solid and the dashed curves are calculated from Eqs. (14), (19) and Eqs. (15)-(17), (19), respectively.

high energy region, it follows that the current-voltage characteristics should be sublinear for the short-range scattering case. The superlinear dependency that is realized in strong fields for scattering on finite-range disorder. Therefore, for intrinsic graphene we obtain unusual combination of the low threshold of nonlinearity and appearance of the second ohmic region for strong fields.

Let us discuss the main assumptions made. Here it is studied intrinsic graphene which has at most resistivity so the effect of heating manifests itself the most. Doped materials require of separate investigation, moreover nonlinearity in these materials must be weaker. We have restricted ourselves by study only of limiting cases of the absence of intercarrier scattering or dominating Coulomb scattering that imposes quasiequilibrium distribution. Point out, that the field dependences of concentration and the current-voltage characteristics there are in good agreement (the strict solution of the problem should be somewhere between the solutions obtained), i.e., they have weak sensitivity to the details of distribution function. As the main generation-recombination mechanism it is assumed radiative-induced interband transitions because Auger-processes are forbidden due to the symmetry of electron-hole states [14]. Possible contribution of

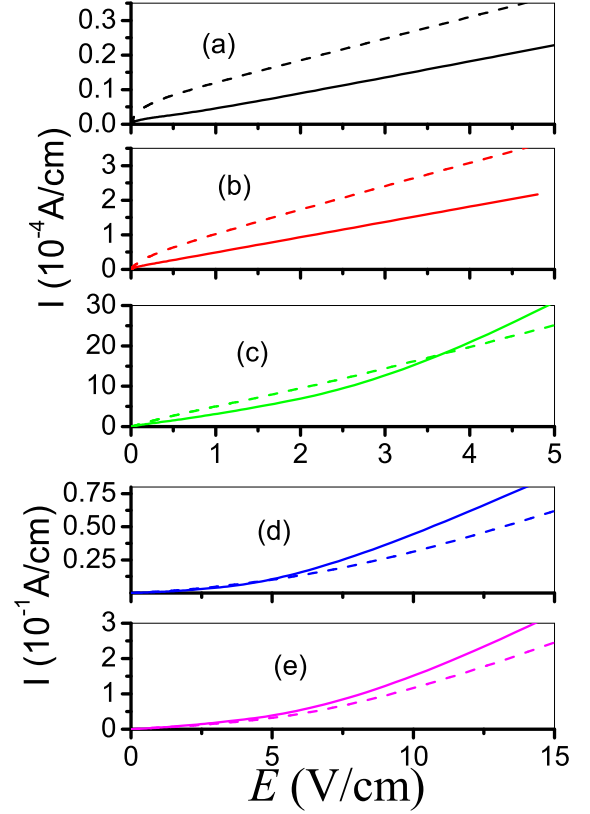


FIG. 8: The same as in Fig. 7 for $l_c = 20$ nm.

other generation-recombination mechanisms (e.g., disorder induced transitions, caused by acoustic phonons or carrier-carrier scattering) demands additional investigation. At last, we consider interaction of carriers with equilibrium thermostat formed by acoustic phonons and radiation (compare with Ref. 18). The problem of heat removal is beyond of the scope of this paper. We speculate now that heat removal is sufficiently effective [7]. In addition, it is possible to use short pulses (all times of relaxation there are $< 1 \mu\text{s}$), when the thermostat will not be overheated. These limitations are related with the lack of data on graphene, however, the qualitative picture will not essentially modify after taking into account with better precision of the parameters and the mechanisms of relaxation.

The rest of assumptions there are standard. To describe the momentum relaxation it is taken into account only the static disorder scattering using the phenomenological model of Ref. 11 (despite that, it corresponds well the experimental data, the microscopic mechanisms of scattering are still unclear [19]) and small contribution of acoustic phonons is discarded. Using of the quasielastic approximation for describing of the energy relaxation is justified by condition $v_W \gg s$, that ensures the small energy transference for the scattering process. As the energy of optical phonons is large, their contribution can be neglected even in considered strong fields.

Also it is unimportant in considered range of the energies an anisotropy of both electron and phonon spectra. Interaction with thermic radiation can be described by taking into account only of direct interband transitions (the Drude absorption is small). Therefore, applied approximations accurately describe the heating mechanism in graphene and lead to correct quantitative estimation of current-voltage characteristics.

In conclusion, prospects of many device applications, in particular, the characteristics of field-effect transistors or effectiveness of graphene interconnections, are substantially dependent on the carries heating. In addition, study of hot electrons (holes) gives information on electron-phonon coupling and about the mechanisms of recombination, i.e., makes possible verification of the relaxation mechanisms. Therefore, we believe that the obtained results will stimulate further experimental and theoretical study (as well as numerical modeling) of hot carriers in graphene.

APPENDIX: KINETIC EQUATION

Below we evaluate the system of quasiclassical kinetic equations governing the nonequilibrium carrier distributions in graphene placed in a strong electric field \mathbf{E} . Such a consideration is analogous to the approach used for the bulk narrow-gap semiconductors, see [20]) and the recent papers [10] which develop a similar approach for the case of graphene. But the case of the bipolar electron-hole plasma is not analyzed in these papers.

We start from the single-particle density matrix which is governed by the quantum kinetic equation [15]:

$$\frac{i}{\hbar} \left[\hat{h}_W - e\mathbf{E} \cdot \mathbf{x}, \hat{\rho} \right] = \hat{J}_{coll}. \quad (\text{A.1})$$

The collision integral \hat{J}_{coll} represents studied above scattering mechanisms and \hat{h}_W is the 2×2 Weyl-Wallash Hamiltonian, [21] describes states nearby the band cross-point. Here we use the linear dispersion laws $\varepsilon_{l\mathbf{p}} = lv_W p$, with l corresponding to the conduction ($l=+1$) or the valence ($l=-1$) bands, the eigenvectors $|l\mathbf{p}\rangle$ are defined from the eigenstate problem:

$$\begin{aligned} \hat{h}_W |l\mathbf{p}\rangle &= \varepsilon_{l\mathbf{p}} |l\mathbf{p}\rangle, & \hat{h}_W &= v_W (\hat{\sigma} \cdot \mathbf{p}), \\ |+\mathbf{1}\mathbf{p}\rangle &= \frac{1}{\sqrt{2}} \begin{pmatrix} 1 \\ e^{i\phi} \end{pmatrix}, & |-\mathbf{1}\mathbf{p}\rangle &= \frac{1}{\sqrt{2}} \begin{pmatrix} -e^{-i\phi} \\ 1 \end{pmatrix}, \end{aligned} \quad (\text{A.2})$$

where ϕ is the \mathbf{p} -plane polar angle. Distribution function over $l\mathbf{p}$ states $F_{l\mathbf{p}} = \langle l\mathbf{p} | \hat{\rho} | l\mathbf{p} \rangle$ and the non-diagonal part of density matrix $\tilde{F}_{\mathbf{p}} = \langle \mathbf{1}\mathbf{p} | \hat{\rho} | -\mathbf{1}\mathbf{p} \rangle = \langle -\mathbf{1}\mathbf{p} | \hat{\rho} | \mathbf{1}\mathbf{p} \rangle^*$ are obtained from the system of kinetic equations:

$$\begin{aligned} e\mathbf{E} \cdot \frac{\partial F_{l\mathbf{p}}}{\partial \mathbf{p}} + l \frac{e}{\hbar} \mathbf{E} \cdot \left\{ \tilde{F}_{\mathbf{p}} \mathbf{X}_{-l,l}(\mathbf{p}) - \mathbf{X}_{l,-l}(\mathbf{p}) \tilde{F}_{\mathbf{p}} \right\} \\ = \langle l\mathbf{p} | J_c(\hat{\rho}) | l\mathbf{p} \rangle \\ \frac{i}{\hbar} 2v_W p \tilde{F}_{\mathbf{p}} + e\mathbf{E} \cdot \frac{\partial \tilde{F}_{\mathbf{p}}}{\partial \mathbf{p}} + \frac{e}{\hbar} \mathbf{E} \cdot \mathbf{X}_{1,-1}(\mathbf{p}) \end{aligned} \quad (\text{A.3})$$

$$\begin{aligned} \times (F_{1\mathbf{p}} - F_{-1\mathbf{p}}) + \frac{e}{\hbar} \mathbf{E} \cdot \{ \mathbf{X}_{-1,-1}(\mathbf{p}) - \mathbf{X}_{1,1}(\mathbf{p}) \} \tilde{F}_{\mathbf{p}} \\ = \langle +\mathbf{1}\mathbf{p} | J_c(\hat{\rho}) | -\mathbf{1}\mathbf{p} \rangle \end{aligned} \quad (\text{A.4})$$

Here the interband matrix element of coordinate, $\mathbf{X}_{l,l'}(\mathbf{p}) = \langle l\mathbf{p} | \hat{x} | l'\mathbf{p} \rangle$, is calculated on wave functions of the momentum representation (A.2) and has the value of the order of \hbar/\bar{p} , where \bar{p} is the characteristic momentum of the hot carries.

In order to show the smallness of nondiagonal components of the distribution function, the estimation $\langle l\mathbf{p} | J_c(\hat{\rho}) | l\mathbf{p} \rangle \sim F_{l\mathbf{p}}/\tau_m$ is also used, where τ_m is the characteristic time of the momentum relaxation (the smallest characteristic time of the problem). For typical conditions of the applicability of quasiclassical description [13]

$$2v_W \bar{p} \gg \frac{\hbar}{\tau_c}, \quad eE\tau_c \ll \bar{p} \quad (\text{A.5})$$

from Eq. (A.4) we have estimation $\tilde{F}_{\mathbf{p}}/F_{l\mathbf{p}} \sim \hbar/(2v_W \bar{p} \tau_c)$.

Further, neglecting by small nondiagonal contributions we arrive to the usual system of kinetic equations:

$$e\mathbf{E} \cdot \frac{\partial F_{l\mathbf{p}}}{\partial \mathbf{p}} = \sum_j J_j \{ F | l\mathbf{p} \}, \quad (\text{A.6})$$

which describes the distribution of hot carriers over the bands $l = \pm 1$ and the 2D momentum \mathbf{p} . The scattering integrals, $J_j \{ F | l\mathbf{p} \}$, are obtained in Ref. [5, 10]. Here l corresponds to conduction ($l=+1$) or valence ($l=-1$) band, \mathbf{p} is the 2D momentum, $J_j \{ F | l\mathbf{p} \}$ is the collision integral for the j th scattering mechanism, [$j = D, LA, R, C$, see discussion after Eq.(1)]. It is convenient to make transition to the electron-hole representation introducing the electron (e) and hole (h) distribution functions, $f_{e\mathbf{p}}$ and $f_{h\mathbf{p}}$, according to the replacements [22]:

$$F_{+1,\mathbf{p}} \rightarrow f_{e\mathbf{p}}, \quad 1 - F_{-1,\mathbf{p}} \rightarrow f_{h\mathbf{p}} \quad (\text{A.7})$$

and to rewrite the collision integrals in (A.6) through $f_{e,h\mathbf{p}}$.

Finally, using the substitution (A.7) and the velocity operator $\hat{\mathbf{v}} = i[\hat{h}_W, \mathbf{x}]/\hbar = v_W \hat{\sigma}$, we obtain the velocity of $l\mathbf{p}$ state: $\langle l\mathbf{p} | \hat{\mathbf{v}} | l\mathbf{p} \rangle = lv_W \mathbf{p}/p \equiv \mathbf{v}_{l\mathbf{p}}$. Taking into account four-fold degeneracy of states in graphene due to spin and valley degrees of freedom, one obtains the current density

$$\mathbf{I} = \frac{4e}{L^2} \sum_{l\mathbf{p}} \mathbf{v}_{l\mathbf{p}} F_{l\mathbf{p}} = \frac{4ev_W}{L^2} \sum_{\mathbf{p}} \frac{\mathbf{p}}{p} (f_{e\mathbf{p}} + f_{h\mathbf{p}}). \quad (\text{A.8})$$

In addition, the intrinsic material the electron density is equal to the hole one (the neutrality condition):

$$\frac{4}{L^2} \sum_{\mathbf{p}} (f_{e\mathbf{p}} - f_{h\mathbf{p}}) = 0. \quad (\text{A.9})$$

Thus, the symmetric scattering for the c - and the v -bands Eqs. (A6), (A8) and (A9) preserve their form

when $f_{e\mathbf{p}}$ is replaced by $f_{h\mathbf{p}}$. Thus, the electron and hole distributions in the intrinsic material are identical,

$f_{e\mathbf{p}} = f_{h\mathbf{p}} \equiv f_{\mathbf{p}}$, so that the kinetic equation and the current density take forms (1) and (3), respectively.

-
- [1] A.H. Castro Neto, F. Guinea, N.M.R. Peres, K.S. Novoselov, and A.K. Geim, *Rev. Mod. Phys.* **81**, 109 (2009).
- [2] P. Avouris, Z. Chen, and V. Perebeinos, *Nature Nanotechnology*, **2**, 605 (2007); P. Avouris, J. Chen, *Materialstoday*, **9** 46 (2006).
- [3] D. Sun, Z.-K. Wu, C. Divin, X. Li, C. Berger, W. A. de Heer, P. N. First, and T. B. Norris, *Phys. Rev. Lett.* **101**, 157402 (2008).
- [4] S. Butscher, F. Milde, M. Hirtschulz, E. Malic, and A. Knorr, *Appl. Phys. Lett.* **91**, 203103 (2007).
- [5] F.T. Vasko and V. Ryzhii, *Phys. Rev. B* **77**, 195433 (2008).
- [6] M.C. Lemme, T.J. Echtermeyer, M. Baus, and H. Kurz, *IEEE Electron Device Lett.* **28** 282 (2007); Y. Q. Wu, P.D. Ye, M.A. Capano, Y. Xuan, Y. Sui, M. Qi, J.A. Cooper, T. Shen, D. Pandey, G. Prakash, and R. Reifengerger, *Appl. Phys. Lett.* **92**, 092192 (2008); X. Wang, Y. Ouyang, X. Li, H. Wang, J. Guo, and H. Dai, arXiv:0803.3464.
- [7] J. Moser, A. Barreiro, and A. Bachtold, *Appl. Phys. Lett.* **91**, 163513 (2007).
- [8] E. H. Hwang, B.Y.-K. Hu, and S. Das Sarma, *Phys. Rev. B* **76**, 115434 (2007); W.-K. Tse, S. Das Sarma arXiv:0812.1008 .
- [9] A. Akturka and N. Goldsman, *J. Appl. Phys.* **103**, 053702 (2008).
- [10] M. Auslender and M. I. Katsnelson, *Phys. Rev. B* **76**, 235425 (2007); S.V. Syzranov, M.V. Fistul, and K.B. Efetov, *Phys. Rev. B* **78**, 045407 (2008).
- [11] F.T. Vasko and V. Ryzhii, *Phys. Rev. B* **76**, 233404 (2007).
- [12] T. Stauber, N. M. R. Peres, and F. Guinea, *Phys. Rev. B* **76**, 205423 (2007); N. M. R. Peres, J. M. B. Lopes dos Santos, and T. Stauber, *Phys. Rev. B* **76**, 073412 (2007); F. Guinea, *Journ. Low Temp. Phys.* **153**, 359 (2008).
- [13] L. Fritz, J. Schmalian, M. Mueller, and S. Sachdev, *Phys. Rev. B* **78**, 085416 (2008); M. Mueller, L. Fritz, and S. Sachdev, *ibid.* **78**, 115406 (2008).
- [14] M.S. Foster and I.L. Aleiner, arXiv:0810.4342.
- [15] F. T. Vasko and O. E. Raichev, *Quantum Kinetic Theory and Applications* (Springer, N.Y. 2005).
- [16] The relation $A_p + p(dA_p/dp)/2 = [d(p^2 A_p)/dp]/2p$ is used in Eq. (8).
- [17] D. Potter, *Computational Physics* (J. Wiley, London, 1973).
- [18] P.N. Romanets, F.T. Vasko, and M.V. Strikha, *Phys. Rev. B* **79**, 033406 (2009).
- [19] T.M. Mohiuddin, L.A. Ponomarenko, R. Yang, S.M. Morozov, A.A. Zhukov, F. Schedin, E.W. Hill, K.S. Novoselov, M.I. Katsnelson, and A. K. Geim, arXiv:0809.1162; S. Adam, P.W. Brouwer, and S. Das Sarma, arXiv:0811.0609.
- [20] I.M. Dykman, V.M. Rosenbaum, and F.T. Vasko, *Phys. Stat. Sol. (b)* **88**, 385 (1978)
- [21] E.M. Lifshitz, L.P. Pitaevskii, and V.B. Berestetskii, *Quantum Electrodynamics*, (Butterworth-Heinemann, Oxford 1982); P.R. Wallace, *Phys. Rev.* **71**, 622 (1947).
- [22] A.I. Anselm, *Introduction to Semiconductor Theory* (Prentice-Hall, Englewood Cliffs, NJ, 1981); since there is no magnetic field under consideration, we do not reverse a momentum direction and the sign of charge ($e < 0$).